2-2013

Removal of Pb(II) from aqueous solution by a zeolite–nanoscale zero-valent iron composite

Seol Ah Kim
Chonbuk National University

Seralathan Kamala-Kannan
Chonbuk National University,

Kui-Jae Lee
Chonbuk National University

Yool-Jin Park
Chonbuk National University

Patrick J. Shea
University of Nebraska - Lincoln, pshea1@unl.edu

See next page for additional authors

Published in *Chemical Engineering Journal* 217 (February 1, 2013), pp. 54-60; doi: 10.1016/j.cej.2012.11.097

Submitted August 11, 2012; revised November 19, 2012; accepted November 21, 2012; published online November 29, 2012.

Removal of Pb(II) from aqueous solution by a zeolite–nanoscale zero-valent iron composite

Seol Ah Kim,[1] Seralathan Kamala-Kannan,[1, 5] Kui-Jae Lee,[1, 5] Yool-Jin Park,[2] Patrick J. Shea,[3] Wang-Hyu Lee,[4, 5] Hyung-Moo Kim,[4, 5] and Byung-Taek Oh [1, 5]

1. Division of Biotechnology, Advanced Institute of Environment and Bioscience, College of Environmental and Bioresource Sciences, Chonbuk National University, Iksan, Jeonbuk 570-752, South Korea
2. Department of Environmental Landscape Architecture-Design, Chonbuk National University, Iksan, Jeonbuk 570-752, South Korea
3. School of Natural Resources, University of Nebraska–Lincoln, Lincoln, NE 68583-0817, USA
4. Department of Agricultural Biology, College of Agricultural and Life Sciences, Chonbuk National University, Jeonju, Jeonbuk 561-756, South Korea
5. Plant Medical Research Center, College of Agricultural and Life Sciences, Chonbuk National University, Jeonju, Jeonbuk 561-756, South Korea

Corresponding authors – H.-M. Kim, Plant Medical Research Center, College of Agricultural and Life Sciences, Chonbuk National University, Jeonju, Jeonbuk 561-756, South Korea; tel 82 63 270 2527, fax 82 63 270 2531, email mc1258@jbnu.ac.kr ; B.-T. Oh, tel 82 63 850 0838, fax 82 63 850 0834, email btoh@jbnu.ac.kr

Co-first authors Seol Ah Kim and Seralathan Kamala-Kannan contributed equally to this work.

Abstract

The effectiveness of nanoscale zero-valent iron (nZVI) to remove heavy metals from water is reduced by its low durability, poor mechanical strength, and tendency to form aggregates. A composite of zeolite and nanoscale zero-valent iron (Z–nZVI) overcomes these problems and shows good potential to remove Pb from water. FTIR spectra support nZVI loading onto the zeolite and reduced Fe^0 oxidation in the Z–nZVI composite. Scanning electron micrographs show aggregation was eliminated and transmission electron micrographs show well-dispersed nZVI in chain-like structures within the zeolite matrix. The mean surface area of the composite was 80.37 m^2/g, much greater than zeolite (1.03 m^2/g) or nZVI (12.25 m^2/g) alone, as determined by BET-N_2 measurement. More than 96% of the Pb(II) was removed from 100 mL of solution containing 100 mg Pb(II)/L within 140 min of mixing with 0.1 g Z–nZVI. Tests with solution containing 1000 mg Pb(II)/L suggested that the capacity of the Z–nZVI is about 806 mg Pb(II)/g. Energy-dispersive X-ray spectroscopy showed the presence of Fe in the composite; X-ray diffraction confirmed formation and immobilization of Fe^0 and subsequent sorption and reduction of some of the Pb(II) to Pb^0. The low quantity of Pb(II) recovered in water-soluble and $Ca(NO_3)_2$-extractable fractions indicate low bioavailability of the Pb(II) removed by the composite. Results support the potential use of the Z–nZVI composite in permeable reactive barriers.

Keywords: Composite, Heavy metals, Nanoscale, Zeolite, Zero-valent iron

1. Introduction

Heavy metals are problematic for ecosystems because of their toxicity and most heavy metals can be highly toxic even at very low concentrations. Among these, Pb is commonly used in several industries and in some locations large amounts of wastewaters containing high concentrations of Pb ions have been released. Lead directly or indirectly reaches surface and ground water and becomes biomagnified in biotic communities. Lead primarily accumulates in muscles, bones, kidneys, and brain tissues and can cause anemia, nervous system disorders, and kidney diseases [1]. Conventional ion exchange, filtration, adsorption, chemical precipitation, and reverse osmosis are being used to remove metals from water [2]. Among these methods, adsorption is a highly efficient and economical removal technique [3].

Permeable reactive barriers (PRBs) are a cost-effective in situ technology for removing a wide array of contaminants from ground water. Optimization of reactive materials remains a major challenge in developing effective PRB technology. Zero-valent iron (ZVI) is being used to remove heavy metals from ground water but low reactivity and handling difficulties have reduced its application in PRBs [4]. Alternatively, nanoscale zero-valent iron (nZVI) has shown good potential to remove metals and other aqueous pollutants. Its physicochemical properties and reductive capacity can facilitate rapid decontamination of polluted water [5, 6]. Unfortunately nZVI often forms aggregates, which decreases efficiency by reducing surface area [7] and producing a less negative oxidation–reduction potential [8]. To resolve this problem, various immobilization techniques are being developed for nZVI stabilization. Wei et al. [7] stabilized nZVI with biodegradable surfactant for effective removal of vinyl chloride and 1,2-dichloroethane from water. Zhang et al. [9] prepared nZVI with pillared clay as a stabilizer for nitrate removal from water. Liu et al. [10] used chitosan to reduce nZVI aggregation and Calabrò et al. [11] prepared nZVI with a pumice granular mixture to remove nickel ions from water.

Zeolites are microporous, aluminosilicate minerals commonly used as adsorbents for several pollutants. Natural zeolites have a high sorption capacity for inorganic pollutants, including heavy metals and ammonium [12]. Basaldella et al. [13] used NaA zeolites to remove Cr from water. Cs and Sr were removed from aqueous solution using zeolite A [14]. Cincotti et al. [15] reported preferential removal of Pb over Cu, Cd and Zn by a Sardinian natural zeolite and Panayotova and Velikov [16] found that Pb(II) was effectively immobilized by Bulgarian natural zeolite. More recently, Yang et al. [17] showed that NKF-6 zeolite effectively removed Pb(II) from a large volume of water. Zeolites have proven effective for environmental applications such as in PRBs for controlling the spread of cation-contaminated groundwater [18]. However, only limited attempts have been made to stabilize nZVI with zeolites for removal of pollutants from water [19]. Lee et al. [19] used a zero-valent iron zeolite material (ZanF) for nitrate reduction without ammonium release under unbuffered pH. ZanF removed the ammonia to below detection limits via adsorption, whereas ZVI alone did not remove it to any significant extent.

The objectives of the present study are to (i) synthesize and characterize a zeolite–nZVI composite (Z–nZVI) and (ii) assess its efficiency for Pb removal. The capacity of Fe^0 as a reductant [20], combined with the properties of zeolite, should promote efficient removal and reduction of Pb(II) to Pb^0.

2. Materials and methods

2.1. Materials and chemicals

Naturally occurring zeolite was obtained from Alfa Aesar, A Johnson Matthey Co., Seoul, South Korea. The zeolite was composed of $Al_2(SiO_3)_3$, Na, Ca, K, and H_2O and had a Mohs hardness of 3.5–5.5. The cation exchange capacity (CEC) of the zeolite was 105.38 $cmol^+/kg$, within the typical range for natural zeolites [12]. After drying at 80 °C overnight, the zeolite was ground and sieved with a 100 mesh screen before use. Ethylenediaminetetraacetic acid (EDTA; DAE JUNG, Siheung, Korea) was >99% pure. All other chemicals were analytical grade. Nanopure water (conductivity = 18 μΩ/m, TOC < 3 μg/L; Barnstead, Waltham, MA, USA) was used to prepare all reagents. A Pb stock solution was prepared by dissolving 1.60 g $Pb(NO_3)_2$ in 100 mL of degassed water and working concentrations were prepared by diluting the stock solution.

2.2. Preparation of the composite

The Z–nZVI composite was prepared according to Wang et al. [21]. Briefly, 1 g of $FeSO_4 \cdot 7H_2O$ and 0.5 g of natural zeolite were mixed in 250 mL of degassed nanopure water. The pH of the solution was adjusted to 4 with 1 M HNO_3. The mixture was treated with ultrasound for 10 min, and then stirred vigorously at ambient temperature for 30 min. To ensure efficient reduction of Fe(II), 25 mL of 1 M KBH_4 solution was added at 30 drops/min while stirring. The reduction reaction is as follows:

$$Fe^{2+} + 2BH_4^- + 6H_2O \rightarrow Fe^0 + 2B(OH)_3 + 7H_2 \uparrow \quad (1)$$

After incubation, the black solids were separated from the solution using a vacuum filtration flask (0.45 μm membrane filter), washed several times with degassed water to remove residual sulfate, then vacuum-dried.

2.3. Characterization of the composite

Field emission scanning electron microscopy (FE-SEM; Hitachi S-4700, Tokyo, Japan) was used to view the morphology and surface characteristics of the nZVI and zeolite. The characteristics of the Z–nZVI composite were obtained using biological transmission electron microscopy (Bio-TEM; Hitachi H-7650, Tokyo, Japan) and energy-dispersive X-ray spectra (EDS) were obtained using FE-SEM. Surface areas of the zeolite, nZVI, and Z–nZVI composite were measured by N_2 adsorption using a Micromeritics ASAP (Accelerated Surface Area and Porosimetry) 2020 analyzer (BELSORP-MINI, BEL Japan, Inc., Osaka, Japan) [6]. Infrared spectra of the zeolite, nZVI, and Z–nZVI composite powders were obtained in KBr pellets on a Perkin–Elmer Fourier transform infrared (FTIR) spectrophotometer (Irvine, CA, USA) in the diffuse reflectance mode at a resolution of 4 cm^{-1}.

2.4. Pb(II) removal and release

The procedures of Zhang et al. [22] were used to determine the effects of initial pH (2–6), temperature (5–60 °C), and Pb(II) concentration (100, 250, 500, and 1000 mg/L) on adsorption to the Z–nZVI composite. The initial pH of the solutions was adjusted using 0.1 M HCl or 0.1 M NaOH but was not controlled during the experiments. Briefly, 0.1 g of the composite was mixed with 100 mL of Pb(II) solution (100 mg/L) and placed on a rotary shaker at 180 rpm and room temperature. Samples were collected periodically up to 140 min and filtered using a 0.45 μm syringe filter. Pb(II) concentration in the filtrate was determined by ICP-AES (Inductively Coupled Plasma, Leeman Labs, Inc., Hudson, NH, USA). Zeolite was used as the control for this experiment.

A sequential extraction procedure was applied to the Pb(II)-loaded Z–nZVI composite to determine Pb(II) availability, following the general procedures of Basta and Gradwohl [23] and Castaldi et al. [24]. To extract readily available Pb(II), Z–nZVI composite (1 g) containing 1.3 mg Pb(II) was shaken with 25 mL of nanopure water (pH 6.8) for 2 h at room temperature (~26 °C). The composite was then sequentially extracted with 25 mL of 0.1 M $Ca(NO_3)_2$ (pH 7.8) to remove exchangeable Pb(II), followed by 25 mL of 0.1 M EDTA (pH 8.0) to remove the more tightly bound Pb(II) or Pb hydroxide complexes precipitated on active sites that were not readily bioavailable [23–25]. After the extractions, the composite was dried overnight at 105 °C and digested with 0.1 M HNO_3 and 0.1 M HCl to recover Pb^0 and other non-exchangeable Pb (likely present as Pb oxides or mixed Pb–Fe oxides). After each extraction the composites were

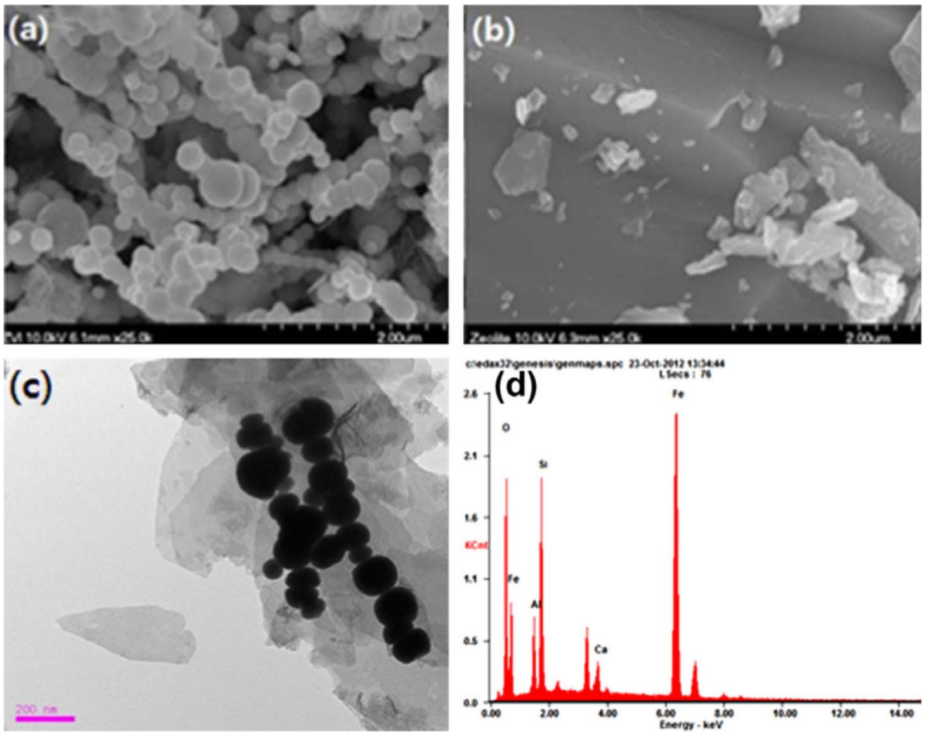

Figure 1. SEM images of (a) nZVI particles and (b) zeolite; TEM image (c) and EDS (d) of the Z–nZVI composite.

centrifuged (6000 rpm for 10 min) and filtered to separate the solution and solid phases [23].

2.5. X-ray diffraction

To determine the nature of the Pb associated with the composite, X-ray diffractograms (XRD) of dried Z–nZVI were obtained after shaking with Pb solution. A Cu Kα incident beam (λ = 0.1546 nm) was used, monochromated by a nickel filtering wave at a tube voltage of 40 kV and current of 40 mA (Philips X'Pert Pro MPD, Eindhoven, Netherlands). Scanning was at a 2θ range of 30–70° at 0.04 deg/min with a time constant of 2 s.

3. Results and discussion

3.1. Characterization of the composite

Typical SEM images of nZVI and zeolite and TEM images of the Z–nZVI composite are shown in Figure 1a–c. As previously reported, nZVI particles become aggregated (attributable to van der Waals and magnetic forces) [7, 26] and the aggregation decreases nZVI reactivity and mobility [27]. Stabilizing supports such as zeolite have been used to prevent aggregation [28]. In our Z–nZVI composite, the zeolite decreased aggregation and the nZVI was present in chain-like structures. EDS further confirmed the presence of Fe in the composite (Figure 1d). The mean surface area of the composite was 80.37 m^2/g, compared to 12.25 m^2/g for nZVI and 1.03 m^2/g for the zeolite alone. The increased surface area of the composite is likely due to non-aggregation of the nZVI particles.

The FTIR spectrum of the Z–nZVI composite supports nZVI loading onto the zeolite. Broad bands at 3400–3600 cm^{-1} in zeolite and the composite (Figure 2b and c) result from O–H stretching, likely due to H_2O and M–OH, while the band at 1650 cm^{-1} can be attributed to O–H bending [29]. The peak at 3500 cm^{-1} and those at 3200, 3100, 3000, 2550 and 2050 cm^{-1} in nZVI can be attributed to the stretching vibrations of O–H groups. Most of these bands disappeared in the composite, indicating loss of water molecules [30, 31]. Bands at 1200–900 cm^{-1} result from SiO_4 and AlO_4 stretching in the zeolite, with bending modes at ca. 740 and 689 cm^{-1} [32, 33]. Major weakening of the zeolite band at 1000 cm^{-1} in the composite and band shifts in this region suggest H-bond breaking due to the presence of Fe on the SiO_4 and AlO_4 surfaces of zeolite [33]. Strong bands at <900 cm^{-1} in the nZVI alone (Figure 2a), attributable in part to iron oxides on the surface [31, 34], are weaker in the composite, indicating less oxidation of zeolite-supported Fe^0. The zeolite support may have reduced Fe (oxy)hydroxide formation, similar to the effect of montmorillonite-supported nZVI [35]. Bands at ~1300 and ~1100 cm^{-1} in the nZVI can be attributed to ethanol used in preparing the sample, but may also include bands associated with sulfate green rust $[Fe^{II}_4Fe^{III}_2(OH)_{12}][SO_4{\cdot}3H_2O]$ [36, 37] and lepidocrocite (γ–FeOOH) [34] formation on some Fe^0 surfaces.

3.2. Removal of Pb(II) from water

Figure 3 shows solution concentrations of Pb(II) as a function of reaction time for 0.1 g of Z–nZVI composite or zeolite in 100 mL of solution containing 100 mg Pb(II)/L at 35 °C. Adjusting the initial pH to 4 dissolved the passivating Fe (oxy) hydroxide layer on nZVI surfaces [38]; the solution pH increased to 7.7 during equilibration due to reaction of nZVI with water [39]. Results indicate that the composite effectively removed 96.2% of the Pb from aqueous solution (96.2 mg/g) within 140 min, while the zeolite alone only removed 39.1% (39.1 mg/g). The enhanced effectiveness of the Z–nZVI composite for Pb(II) removal is likely due to its much larger specific surface area than that of zeolite alone. The zeolite supporting material prevented aggregation of nZVI, thereby providing more surface area for Pb(II) sorption [31]. Results are consistent with previous studies reporting adsorption of Pb(II) by kaolinite-supported nZVI, and Cr(VI) and Pb(II) adsorption by resin-supported nZVI [31, 40].

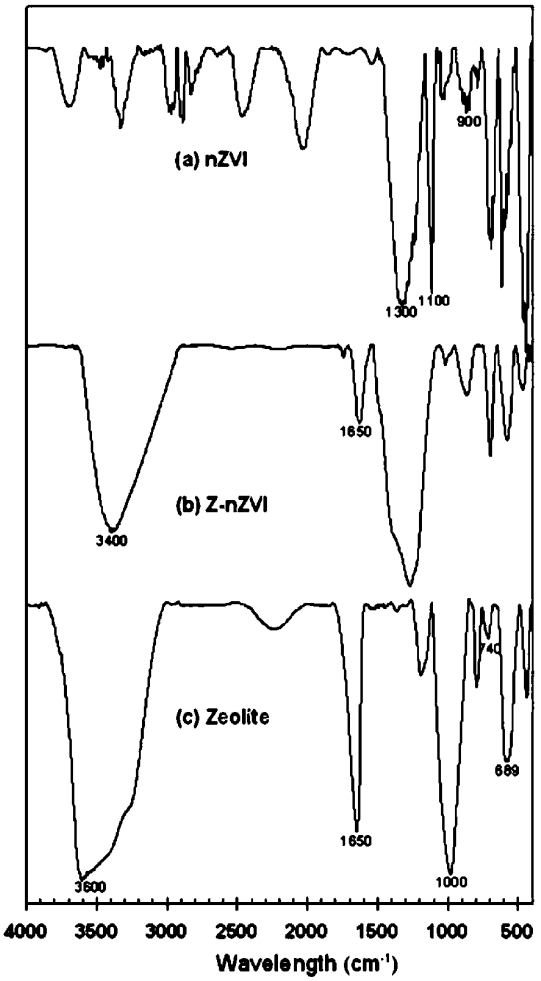

Figure 2. FT-IR spectra of (a) nZVI, (b) Z–nZVI, and (c) zeolite.

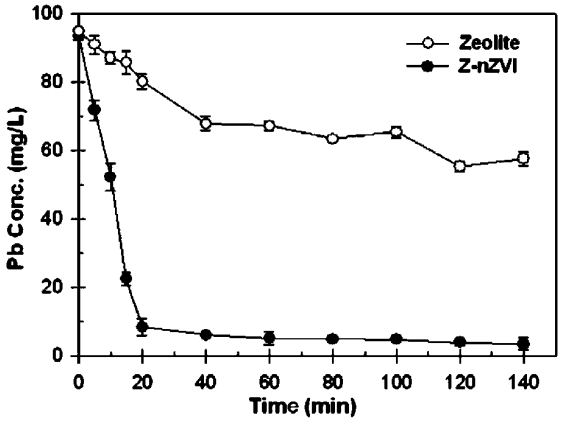

Figure 3. Removal of Pb(II) by 0.1 g of Z–nZVI compared to zeolite alone after shaking with 100 mL of aqueous solution containing 100 mg Pb(II)/L for 140 min at pH 4 and 35 °C. Error bars indicate standard deviations of the means; where absent, bars fall within symbols.

3.2.1. *Effect of Pb(II) concentration*

The effect of initial Pb(II) concentration (100–1000 mg/L) on removal efficiency was investigated by shaking 0.1 g of the composite in 100 mL of solution for 140 min at 35 °C and an initial pH of 4. Removal efficiency varied with initial concentration (Figure 4). At the lower concentration (100 mg/L), 99.2% of the Pb(II) was removed by the Z–nZVI composite (99.2 mg/g). The decrease in removal efficiency to 80.6% at the higher concentration (1000 mg/L) suggests that the capacity of the Z–nZVI is about 806 mg Pb(II)/g, which was exceeded under the conditions of the experiment, as observed for removal of Pb(II), Cu(II), and Zn(II) by natural zeolite [41] and Cr(VI) ions by a bentonite–nZVI composite [42].

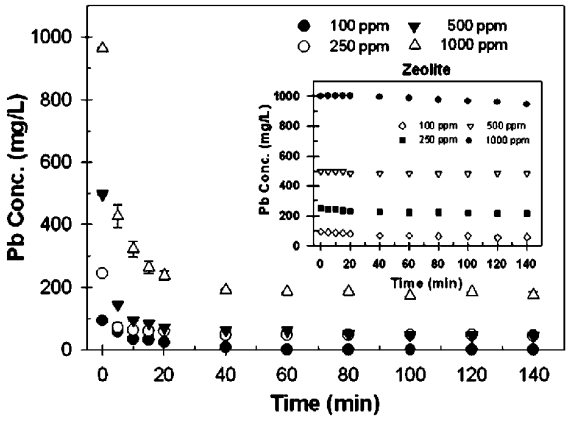

Figure 4. Effect of initial concentration on Pb(II) removal by 0.1 g of Z–nZVI after shaking with 100 mL of aqueous solution for 140 min at pH 4 and 35 °C. Error bars indicate standard deviations of the means; where absent, bars fall within symbols. The insert shows Pb(II) removal efficiency by zeolite.

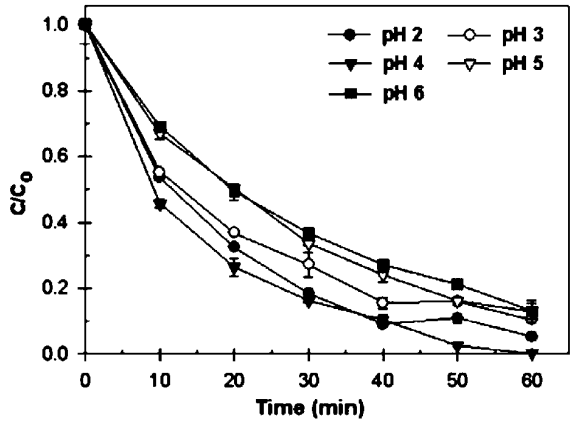

Figure 5. Effect of initial pH on Pb(II) removal by 0.1 g Z–nZVI from 100 mL of aqueous solution containing 100 mg Pb(II)/L after shaking for 60 min at room temperature (26 ± 2 °C). Error bars indicate standard deviations of the means; where absent, bars fall within symbols.

3.2.2. *Effect of initial pH*

Solution pH can have a significant influence on the adsorption of heavy metals, due to metal speciation, surface charge, and functional group chemistry of the adsorbent [43]. Hence, 0.1 g of the Z–nZVI composite was mixed with 100 mL of solution containing 100 mg Pb(II)/L at an initial pH of 2–6 (26 ± 2 °C). The pH of the solutions was adjusted before adding the Z–nZVI composite, but increased from 2 to 6.1, 3 to 7.4, 4 to 7.7, 5 to 8.2 and 6 to 7.8 during the experiment, primarily from oxidation of Fe^0 (and Fe^{2+}) by water [39]. Varying the initial pH had a small effect on Pb(II) removal efficiency (Figure 5); removal ranged from 99.9% when the initial pH was 4–93.5% when it was 6. The difference in pH would have a minimal effect on the surface charge of zeolite [44]. Although Pb^{2+} ions predominate in solution at acidic

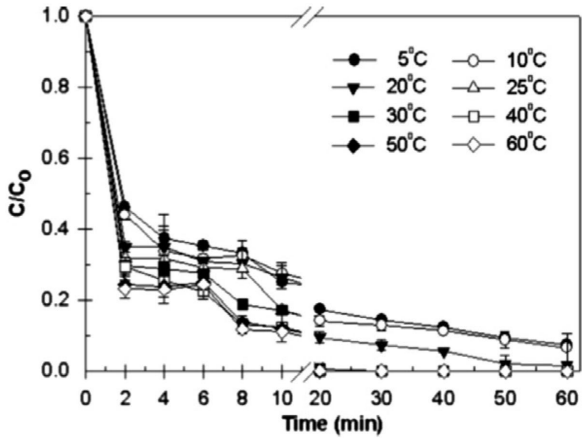

Figure 6. Effect of temperature on Pb(II) removal by 0.1 g Z–nZVI from 100 mL of aqueous solution containing 100 mg Pb(II)/L. Error bars indicate standard deviations of the means; where absent, bars fall within symbols.

pH, competition from protons decreases removal at an initial pH of 2 [22]. Conversely, when the initial pH was 6 the presence and adsorption of $Pb(OH)^+$ may have prevented Pb^{2+} diffusion to some sites within the porous zeolite structure [41]. The greater Fe (oxy)hydroxide coating on nZVI surfaces at an initial pH of 6 would also decrease reactivity, reflected in a smaller pH change during the experiment. Our results suggest that rapid diffusion of Pb^{2+} into the Z–nZVI matrix and adsorption were optimized by adjusting the initial pH to 4, and were followed by reduction to Pb^0 by Fe^0. The more acidic solution pH facilitates these processes through dissolution of the passivating Fe (oxy)hydroxide layer on nZVI surfaces [38]. While aggregation of nZVI may increase near its effective point of zero charge, which likely ranged from 6–8 due to surficial Fe (oxy)hydroxides, most of the Fe^0 is immobilized on zeolite in the Z–nZVI composite.

3.2.3. Effect of temperature

Temperature is an important factor affecting adsorption and would be generally expected to increase with decreasing temperature due to the exothermicity of cations for an adsorbent surface. Temperature had a relatively small effect on Pb removal by the Z–nZVI composite, which ranged from 99.8% at 60 °C to 94.6% at 5 °C (Figure 6). More efficient removal at higher temperatures is likely due to desolvation of Pb cations [17] and more rapid diffusion into the internal pores of the composite particles. Results are consistent with the greater adsorption of Pb(II) on NKF-6 zeolite [17] and Cr(VI) on a bentonite-nZVI composite [42] with increasing temperature.

3.2.4. X-ray diffraction

XRD patterns of the Z–nZVI composite were recorded before and after shaking with the aqueous solution alone (Figures 7a and b, respectively) or with the Pb solution (Figure 7c). Peak 1 (and 4) at $2\theta \sim 32$ likely arises from SiO_2 associated with the natural zeolite [45], while that at $2\theta = 45$ (2 and 12) is characteristic of Fe0 [33; JCPDS00-006-0696]. Fe(II) adsorbed to the zeolite was likely reduced to Fe^0 and immobilized on the surface, as described by Lee et al. [19]. Peak 3 ($2\theta = 50$) is likely due to maghemite (γ-Fe_2O_3) on some of the Fe^0 [46]. Peaks 5–10, appearing in Z–nZVI after shaking with aqueous solution, can be attributed to the formation of iron oxides, primarily magnetite (Fe_3O_4), maghemite, and lepidocrocite from Fe^0 oxidation [31]. The peaks at $2\theta \sim 35$ (11) and ~ 62 (14)

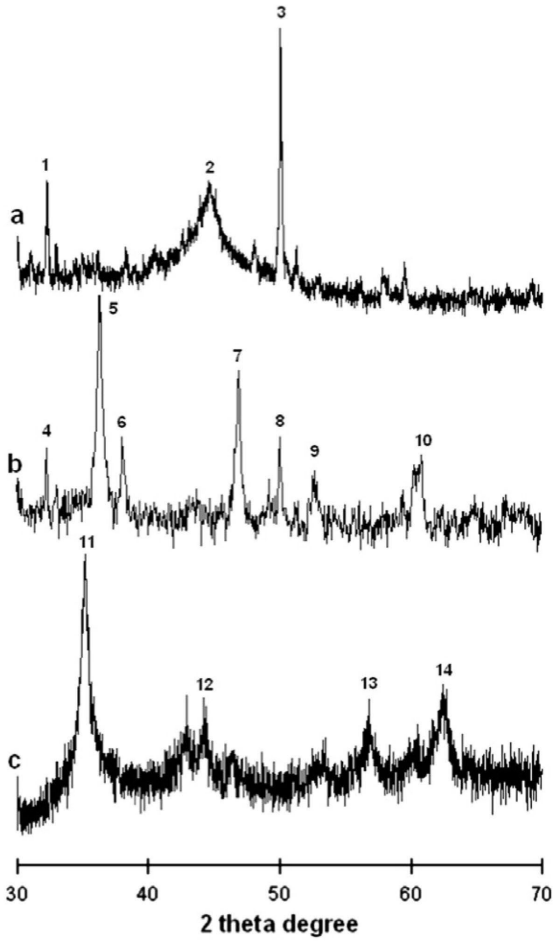

Figure 7. XRD patterns of (a) the Z–nZVI; (b) Z–nZVI after shaking with aqueous solution alone; and (c) Z–nZVI after shaking with aqueous solution containing 250 mg Pb(II)/L. 1,4 = SiO_2; 2,12 = Fe^0; 3,8 = γ-Fe_2O_3; 5–10, 13 = iron oxides; 11,14 = Pb^0.

Table 1. Release of lead by sequential extraction of 1 g of Pb-containing Z–nZVI composite with 25 mL of H_2O, 0.1 M $Ca(NO_3)_2$, and 0.1 M EDTA.

Extractant	Pb (μg)	% of total
Initial amount in the Z–nZVI composite	1303.25 ± 0.03	100.0
H_2O	5.30 ± 0.08	0.4
$Ca(NO_3)_2$ (0.1 M)	29.45 ± 6.73	2.3
EDTA (0.1 M)	1074.50 ± 6.18	82.5
Digestion of Z–nZVI with HNO_3/HCl	193.05 ± 57.28	14.8

in the Z–nZVI composite after exposure to Pb(II) solution (Figure 7c) are attributed to Pb^0 [31, 40], while that at $2\theta \sim 57$ (13) is likely an iron oxide. The XRD analyses support formation and immobilization of Fe^0, as well as sorption and reduction of Pb(II) to Pb^0, on the composite.

3.3. Availability of Pb removed by the composite

The Pb(II)-loaded composite was sequentially shaken with extractant solutions of increasing removal capacity to determine the availability of Pb associated with the composite. Lead readily extractable with water comprises the most soluble and bioavailable fraction. That fraction was less than 0.5% of the adsorbed Pb(II) (Table 1). The fraction extractable with $Ca(NO_3)_2$ comprised exchangeable Pb, which was about 2.3% of the Pb initially removed by the Z–nZVI composite. In contrast, the fraction extracted with EDTA, consid-

ered as not readily bioavailable [23–25], was 82.5% of the adsorbed Pb(II). The residual fraction, which is not expected to be readily released under natural conditions, comprised 14.8% of the Pb(II) associated with the composite. Aside from Pb^0 resulting from Pb(II) reduction, this fraction may include some Pb replaced for Al within the zeolite lattice [24].

The low quantity of Pb(II) recovered in the water-soluble and $Ca(NO_3)_2$-extractable fractions (Table 1) indicates low bioavailability of the Pb removed by the Z–nZVI composite. These fractions likely consist of Pb^{2+} electrostatically adsorbed to external surfaces of the composite [24]. The large fraction of Pb(II) extracted with EDTA likely consists of more strongly bound Pb(II) and precipitated lead hydroxide complexes on active sites within the zeolite-based matrix of the composite [41, 44]. EDTA is known to be highly effective for extracting lead from soil and the Pb–EDTA complex has high stability at pH 8 [47], the pH of the EDTA solution in our experiment. Our results suggest that a large fraction of the Pb(II) removed by the Z–nZVI was incorporated into the internal matrix of the composite. We postulate that the nZVI within the composite sequestered the Pb(II) and gradually reduced it to Pb^0, as described for adsorption and reduction of Ni(II) by nZVI [48]. Once the metal becomes incorporated within the composite structure, it remains essentially insoluble and non-exchangeable [24].

4. Conclusions

Zeolite was an effective dispersant and stabilizer of nZVI in a composite support system, reducing aggregation and increasing specific surface area. Batch experiments indicated that the Z–nZVI composite was superior to zeolite in removing Pb(II) from aqueous solution. XRD confirmed that the composite adsorbed the Pb(II) ions and subsequently reduced some of them to Pb^0. Because zeolite is a stable and low-cost mineral, the zeolite–nZVI composite is an efficient and promising reactive material for PRBs. Further studies are needed to assess the potential of the material to remove other metals and organic pollutants.

Acknowledgment — This paper was supported by research funds of Chonbuk National University for 2010 Campus Faculty Exchange Program.

References

[1] US EPA, Cost and benefits of reducing lead in gasoline, Draft final report, Office of policy analysis, US EPA 230-03-84-005, Washington, DC, 1984.

[2] F. Fu, Q. Wang, Removal of heavy metal ions from wastewaters: A review, J. Environ. Manage. 92 (2011) 407–418.

[3] M.K. Mondal, Removal of Pb(II) ions from aqueous solution using activated tea waste: Adsorption on a fixed-bed column, J. Environ. Manage. 90 (2009) 3266– 3271.

[4] K.J. Lee, Y. Lee, J. Yoon, S. Kamala-Kannan, S.M. Park, B.T. Oh, Assessment of zero-valent iron as a permeable reactive barrier for long-term removal of arsenic compounds from synthetic water, Environ. Technol. 30 (2009) 1425– 1434.

[5] X.Q. Li, D.W. Elliott, W.X. Zhang, Zero-valent iron nanoparticles for abatement of environmental pollutants: Materials and engineering aspects, Crit. Rev. Solid State Mater. Sci. 31 (2006) 111–122.

[6] Y.P. Sun, X.Q. Li, J. CaO, W.X. Zhang, H.P. Wang, Characterization of zero-valent iron nanoparticles, Adv. Colloid Interface Sci. 120 (2006) 47–56.

[7] Y.T. Wei, S.C. Wu, S.W. Yang, C.H. Che, H.L. Lien, D.H. Huang, Biodegradable surfactant stabilized nanoscale zero-valent iron for in situ treatment of vinyl chloride and 1,2-dichloroethane, J. Hazard. Mater. 211–212 (2012) 373–380.

[8] Z. Shi, J.T. Nurmi, P.G. Tratnyek, Effects of nano zero-valent iron on oxidation reduction potential, Environ. Sci. Technol. 45 (2011) 586–1592.

[9] Y. Zhang, Y. Li, J. Li, L. Hu, X. Zheng, Enhanced removal of nitrate by a novel composite: Nanoscale zero valent iron supported on pillared clay, Chem. Eng. J. 171 (2011) 526–531.

[10] T. Liu, Z.L. Wang, L. Zhao, X. Yang, Enhanced chitosan/Fe^0-nanoparticles beads for hexavalent chromium removal from wastewater, Chem. Eng. J. 189–190 (2012) 196–202.

[11] P.S. Calabro, N. Moraci, P. Suraci, Estimate of the optimum weight ratio in zerovalent/ pumice granular mixtures used in permeable reactive barriers for the remediation of nickel contaminated groundwater, J. Hazard. Mater. 207–208 (2012) 111–116.

[12] S. Wang, Y. Peng, Natural zeolites as effective adsorbents in water and wastewater treatment, Chem. Eng. J. 156 (2010) 11–24.

[13] E.I. Basaldella, P.G. Vazquez, F. Iucolano, D. Caputo, Chromium removal from water using LTA zeolites: Effect of pH, J. Colloid Interface Sci. 313 (2007) 574– 578.

[14] A.M. EI-Kamash, Evaluation of zeolite A for the sorptive removal of Cs^+ and Sr^{2+} ions from aqueous solutions using batch and fixed bed column operations, J. Hazard. Mater. 151 (2008) 432–445.

[15] A. Cincotti, A. Mameli, A.M. Locci, R. Orru, G. Cao, Heavy metal uptake by Sardinian natural zeolites: Experiment and modeling, Ind. Eng. Chem. Res. 45 (2006) 1074–1084.

[16] M. Panayotova, B. Velikov, Kinetics of heavy metal ions removal by use of natural zeolite, J. Environ. Sci. Health A 37 (2002) 139–147.

[17] X. Yang, S. Yang, S. Yang, J. Hu, X. Tan, X. Wang, Effect of pH, ionic strength and temperature on sorption of Pb(II) on NKF-6 zeolite studied by batch technique, Chem. Eng. J. 168 (2011) 86–93.

[18] J.B. Park, S.H. Lee, J.W. Lee, C.Y. Lee, Lab scale experiments for permeable reactive barriers against contaminated groundwater with ammonium and heavy metals using clinoptilolite (01-29B), J. Hazard. Mater. B95 (2002) 65–79.

[19] S. Lee, K. Lee, S. Rhee, J. Park, Development of a new zero-valent iron zeolite material to reduce nitrate without ammonium release, J. Environ. Eng. 133 (2007) 6–12.

[20] W.M. Haynes, Handbook of Chemistry and Physics, 92nd ed., CRC Press, Boca Raton, FL, USA, Internet Version 2012; http://www.hbcpnetbase.com

[21] W. Wang, M. Zhou, Q. Mao, J. Yue, X. Wang, Novel NaY zeolite-supported nanoscale zero-valent iron as an efficient heterogeneous Fenton catalyst, Catal. Commun. 11 (2010) 937–941.

[22] X. Zhang, S. Lin, X.Q. Lu, Z.L. Chen, Removal of Pb(II) from water using synthesized kaolin supported nanoscale zero-valent iron, Chem. Eng. J. 163 (2010) 243–248.

[23] N.T. Basta, R. Gradwohl, Estimation of Cd, Pb, and Zn bioavailability in smelter-contaminated soils by a sequential extraction procedure, J. Soil Contam. 9 (2000) 149–164.

[24] P. Castaldi, L. Santona, S. Enzo, P. Melis, Sorption processes and XRD analysis of a natural zeolite exchanged with Pb^{2+}, Cd^{2+} and Zn^{2+} cations, J. Hazard. Mater. 156 (2008) 428–434.

[25] N.T. Basta, R. Gradwohl, K.L. Snethen, J.L. Schroder, Chemical immobilization of lead, zinc, and cadmium in smelter-contaminated soils using biosolids and rock phosphate, J. Environ. Qual. 30 (2001) 1222–1230.

[26] F. He, D. Zhao, J. Liu, C.B. Roberts, Stabilization of Fe–Pd nanoparticles with sodium carboxymethyl cellulose for en-

hanced transport and dechlorination of trichloroethylene in soil and groundwater, Ind. Eng. Chem. Res. 46 (2007) 29– 34.

[27] Y. Liu, T. Phenrat, G.V. Lowry, Effect of TCE concentration and dissolved groundwater solutes on NZVI-promoted TCE dechlorination and H_2 evolution, Environ. Sci. Technol. 41 (2007) 7881–7887.

[28] C. Uzum, T. Shahwan, A.E. Eroğlu, K.R. Hallam, T.B. Scott, I. Lieberwirth, Synthesis and characterization of kaolinite-supported zero-valent iron nanoparticles and their application for the removal of aqueous Cu^{2+} and Co^{2+} ions, Appl. Clay Sci. 43 (2009) 172–181.

[29] M. Mohapatra, L. Mohapatra, P. Singh, S. Anand, B.K. Mishra, A comparative study on Pb(II), Cd(II), Cu(II), Co(II) adsorption from single and binary aqueous solutions on additive assisted nano-structured goethite, Int. J. Eng. Sci. Technol. 2 (2010) 89–103.

[30] V.I. Portilla, The nature of hydrogen bonds and water in legrandite by IR spectroscopy, Am. Mineral. 61 (1976) 95–99.

[31] X. Zhang, S. Lin, Z. Chen, M. Megharaj, R. Naidu, Kaolinite-supported nanoscale zero-valent iron for removal of Pb^{2+} from aqueous solution: reactivity, characterization and mechanism, Water Res. 45 (2011) 3481–3488.

[32] B.I. Shikunov, L.I. Lafer, V.I. Yakerson, I.V. Mishin, A.M. Rubinshtein, Infrared spectra of synthetic zeolites, Izvestiya Akademii Nauk SSSR, Seriya Khimicheskaya 1 (1972) 204–206.

[33] M.E. Canafoglia, I.D. Lick, E.N. Ponzi, I.L. Botto, Natural materials modified with transition metals of the cobalt group: Feasibility in catalysis, J. Argentine Chem. Soc. 97 (2009) 58–68.

[34] A.L. Andrade, D.M. Souza, M.C. Pereira, J.D. Fabris, R.Z. Domingues, Synthesis and characterization of magnetic nanoparticles coated with silica through a sol–gel approach, Ceramica 55 (2009) 420–424.

[35] P. Yuan, M. Fan, D. Yang, H. He, D. Liu, A. Yuan, J. Zhu, T. Chen, Montmorillonite-supported magnetite nanoparticles for the removal of hexavalent chromium [Cr(VI)] from aqueous solutions, J. Hazard. Mater. 166 (2009) 821–829.

[36] S.M. Ponder, J.G. Darab, J. Bucher, D. Caulder, I. Craig, L. Davis, N. Edelstein, W. Lukens, H. Nitsche, L. Rao, D.K. Shuh, T.E. Mallouk, Surface chemistry and electrochemistry of supported zero-valent iron nanoparticles in the remediation of aqueous metal contaminants, Chem. Mater. 13 (2001) 479– 486.

[37] M. Gotić, S. Musić, Mossbauer, FT-IR and FE SEM investigation of iron oxides precipitated from $FeSO_4$ solutions, J. Mol. Struct. 834–836 (2007) 445–453.

[38] L. Selwyn, Overview of archaeological iron: the corrosion problem, key factors affecting treatment, and gaps in current knowledge, in: J. Ashton, Hallam (Eds.), Metal 2004: Proceedings of Interim Meeting of the ICOM-CC Metal WG, National Museum of Australia, Canberra, pp. 294–306.

[39] W-X. Zhang, Nanoscale iron particles for environmental remediation: A review, J. Nanoparticle Res. (2003) 323–332.

[40] S.M. Ponder, J.G. Darab, T.E. Mallouk, Remediation of Cr(VI) and Pb(II) aqueous solutions using supported, nanoscale zero-valent iron, Environ. Sci. Technol. 34 (2000) 2564–2569.

[41] J. Perić, M. Trgo, N. Vukojević Medvidović, Removal of zinc, copper and lead by natural zeolite – A comparison of adsorption isotherms, Water Res. 38 (2004) 1893–1899.

[42] L.N. Shi, X. Zhang, Z.L. Chen, Removal of chromium(VI) from wastewater using bentonite-supported nanoscale zero-valent iron, Water Res. 45 (2011) 886– 892.

[43] G. Crini, H.N. Peindy, F. Gimbert, C. Robert, Removal of C.I. Basic Green 4 (malachite green) from aqueous solutions by adsorption using cyclodextrinbased adsorbent: Kinetic and equilibrium studies, Sep. Purif. Technol. 53 (2007) 97–110.

[44] A. Ponizovsky, C.D. Tsadilas, Lead(II) retention by Alfisol and clinoptilolite: Cation balance and pH effect, Geoderma 115 (2003) 303–312.

[45] S.A. Ibitoye, A.A.A. Afonja, Characterization of cold briquetted iron (CBI) by X-ray diffraction technique, J. Min. Mater. Charact. Eng. 7 (2007) 39–48.

[46] J. Drbohlavova, R. Hrdy, V. Adam, R. Kizek, O. Schneeweiss, J. Hubalek, Preparation and properties of various magnetic nanoparticles, Sensors 9 (2009) 2352–2362.

[47] C. Kim, Y. Lee, S.K. Ong, Factors affected EDTA extraction of lead from lead-contaminated soils, Chemosphere 51 (2003) 845–853.

[48] X.-Q. Li, Q.-X. Zhang, Iron nanoparticles: The core–shell structure and unique properties for Ni(II) sequestration, Langmuir 22 (2006) 4638–4642.